

# Amygdalin Delays Cartilage Endplate Degeneration and Improves Intervertebral Disc Degeneration by Inhibiting NF- $\kappa$ B Signaling Pathway and Inflammatory Response

Qinghe Zeng<sup>1,2,\*</sup>, Qi Sun<sup>3,\*</sup>, Huihui Xu<sup>1,2,\*</sup>, Jiali Chen<sup>1</sup>, Houfu Ling<sup>4</sup>, Qinwen Ge<sup>1,2</sup>, Kaiao Zou<sup>1,2</sup>, Xu Wang<sup>1,2</sup>, Hongting Jin<sup>1</sup>, Ju Li<sup>4,\*</sup>, Minwei Jin<sup>4,\*</sup>

<sup>1</sup>Institute of Orthopedics and Traumatology, the First Affiliated Hospital of Zhejiang Chinese Medical University, Zhejiang Provincial Hospital of Chinese Medicine, Zhejiang Chinese Medical University, Hangzhou, People's Republic of China; <sup>2</sup>The First College of Clinical Medicine, Zhejiang Chinese Medical University, Hangzhou, People's Republic of China; <sup>3</sup>Department of Orthopaedic Surgery, Fuyang Orthopaedics and Traumatology Affiliated Hospital of Zhejiang Chinese Medical University, Hangzhou, Zhejiang, People's Republic of China; <sup>4</sup>Department of Orthopaedics, The First Affiliated Hospital of Zhejiang Chinese Medical University, Hangzhou, People's Republic of China

\*These authors contributed equally to this work

Correspondence: Minwei Jin; Ju Li, Email jin872@zcmu.edu.cn; juli@zcmu.edu.cn

**Background:** Intervertebral disc degeneration (IDD) is a major cause of lower back pain (LBP), in which inflammatory is frequently involved. Amygdalin (AMD) is a naturally occurring compound that exerts anti-fibrotic, anti-inflammatory, analgesic, and immunomodulatory effects in various diseases. The purpose of this study was to investigate the therapeutic effects and molecular mechanisms of AMD on Lumbar spine instability (LSI)-induced IDD in mice.

**Methods:** In this study, we first explored the effects of AMD in vivo, and then further explored the mechanism of its effects both in vivo and in vitro. Ten-week-old male C57BL/6J mice were administrated with AMD. At 10 weeks after LSI, spinal were collected for tissue analyses, including histology, micro-CT, and immunohistochemistry for Col2, Mmp-13, TNF- $\alpha$ , and p-P65. Additionally, we also evaluated the mRNA and protein expression level of p-P65 and p-IKB $\alpha$  after being treated with AMD in vitro.

**Results:** Histological staining, micro-CT and immunohistochemical analysis showed that AMD treatment significantly inhibited the expression of TNF- $\alpha$  and Mmp-13, increased the expression of Col2 as well as attenuated the calcification of cartilage endplates, eventually to delayed the progression of IDD. Meanwhile, in vivo and in vitro fluorescence imaging revealed that AMD markedly inhibited the AMD significantly inhibited the LSI-induced increase in TNF- $\alpha$  expression and P65 and IKB $\alpha$  phosphorylation.

**Discussion:** Our findings suggest that AMD partly inhibits the activation of NF- $\kappa$ B signaling pathway to reduce the release of inflammatory mediators and delay the degeneration of cartilage endplate in IDD model mice. Therefore, AMD may be a potential candidate for the treatment of IDD.

**Keywords:** intervertebral disc degeneration, amygdalin, cartilage endplate, inflammatory processes, NF- $\kappa$ B pathway

## Introduction

Low back pain (LBP) is one of the common orthopaedic diseases in daily life, and its prevalence is increasing with age, and it is also related to excessive exercise.<sup>1,2</sup> This not only affects people's quality of life but also increases the burden of social medical resources.<sup>3</sup> As research has found, disc degeneration is closely linked to LBP and is one of the main causes of LBP.<sup>4</sup> However, the exact mechanism of Intervertebral disc degeneration (IDD) has not yet been elucidated.<sup>5</sup> The intervertebral disc (IVD) is a fibrocartilaginous disc between two adjacent pyramids, consisting of the nucleus pulposus (NP), the annulus fibrosus (AF), and the upper and lower cartilage endplates (CEP). Modern studies have found that IDD is mainly manifested in the reduction of the number of NP cells, abnormal ECM metabolism, reduction of type

II collagen, and calcification and death of endplate chondrocytes, etc.<sup>6</sup> Nowadays, the therapeutic strategies to treat IVD degeneration and assuage IDD-related pain include conservative treatments, such as anti-inflammatory drugs. When these treatments prove themselves inefficient, radical surgical interventions (eg disc removal and spinal fusion) are considered. These changes are closely related to the inflammatory response mediated by cellular inflammatory factors. Inflammation not only reduces the synthesis of extracellular matrix such as proteoglycans and type II collagen but also promotes the expression of matrix metalloproteinases (MMPs), which further reduces the biological properties of cartilage endplates and eventually leads to IDD.<sup>7–9</sup> For example, administration of Chlorogenic Acid (CGA) mitigated cartilaginous endplate degeneration and postponed IDD development accompanying a decrease of inflammatory and catabolic mediators.<sup>10</sup>

The Nuclear Factor- $\kappa$ B (NF- $\kappa$ B) transcription factor has long-term been considered as a causative factor of IDD, NF- $\kappa$ B signaling is very important for maintenance of IVD homeostasis.<sup>11,12</sup> In the process of IDD, multiple factors (inflammation, oxidative stress, mechanical loading, etc.) activating NF- $\kappa$ B signaling induce the expression of matrix degrading enzymes, thus accelerating the catabolism of ECM.<sup>13,14</sup> Activation of the NF- $\kappa$ B signaling pathway can increase the expression levels of many inflammatory mediators and chemokines, creating a vicious cycle and further accelerating the progression of IDD.<sup>15</sup> It has been shown that knockdown by injection of specific NF- $\kappa$ B p65 siRNA in an NP degeneration model reduces degeneration of NP caused by injury.<sup>16</sup> However, the effect of NF- $\kappa$ B signaling on cartilage endplates is unclear.

Amygdalin (AMD), also known as vitamin B17, is one of the main pharmacological components in almonds and is widely distributed in the seeds of Rosaceae plants such as peach, plum, apple, and bayberry.<sup>17,18</sup> The pharmacological activities of AMD have been well documented over the years, including anti-fibrotic, anti-inflammatory, analgesic, and immunomodulatory.<sup>19–22</sup> More importantly, AMD exerts anti-inflammatory effects by inhibiting the expression of inflammatory factors and regulating NF- $\kappa$ B signaling pathway.<sup>23,24</sup> Likewise, AMD has been reported to inhibit LPS-induced TNF- $\alpha$  and IL-1 $\beta$  mRNA expression and alleviate carrageenan-induced arthritis in rats.<sup>21</sup> Meantime, AMD could inhibit the degeneration of the endplate chondrocytes derived from intervertebral discs of rats induced by IL-1 $\beta$ .<sup>25</sup> Therefore, the above findings suggest that AMD may exert a chondroprotective effect by inhibiting the inflammatory response.

Based on the above studies, we hypothesized that AMD could ameliorate inflammation-related chondrocyte pathological changes and serve as a potential drug therapy for IDD. In the present study, we evaluated the therapeutic effect of AMD in IDD and explored its potential mechanism of action through in vivo and in vitro experiments.

## Materials and Methods

### Animals

18 10-week-old male C57BL / 6J mice were provided by the Animal Center of Zhejiang University of Traditional Chinese Medicine (Hangzhou). NF- $\kappa$ B-GFP-luciferase (NGL) mice used for cellular localization of NF- $\kappa$ B activation and quantification were purchased from Jackson Laboratory (Bar Harbor, Maine, USA). All mice in this study were housed in the pathogen-free laboratory of Zhejiang University of Traditional Chinese Medicine Animal Center (Hangzhou), with 6 mice per cage, and had free access to clean food and water. All experiments were carried out after being approved by the Animal Experiment Ethics Committee of Zhejiang University of Traditional Chinese Medicine (Hangzhou) and complied with the guidelines of the Care and Use of Laboratory Animals (LZ12H27001).

### Experimental Grouping and Administration

The experimental mice were randomly divided into a sham operation group (Sham), a Lumbar spine instability (LSI) model group (LSI), and an Amygdalin group (Amygdalin, CAS NO. 29883–15-6, purity  $\geq$  97.0%, Sigma, St. Louis, MO, USA). Six mice were sampled 12 weeks after surgery. According to previous studies, a mouse model of lumbar instability was used to induce IDD in lumbar spine degeneration surgery.<sup>26,27</sup> That is, mice anesthetized with sodium pentobarbital were placed in a prone position, and the supraspinous ligament, interspinous ligament, and spinous process between the second and sixth lumbar vertebrae were freed, the supraspinous ligament, interspinous ligament and spinous process between the third lumbar vertebrae to the fifth lumbar vertebrae were then removed with a machete. At the same

time, only the paraspinal muscle tissue was removed from the mice in the sham operation group, and the sampling time of the mice was the same as that of the mice in the operation group. Finally, the incision was closed with antibiotics to prevent infection, and the mice were returned to the cage. Mice in the amygdalin group received AMD (0.1 mg/kg) intraperitoneal injection from the 4th week after LSI, once a day for 8 weeks. The sham operation group and the model group were given the same amount of normal saline at the same time.

## DigiGait Imaging System Analysis

The Gait of the mice in each group was recorded and analyzed with the DigiGait imaging system. Measurements were taken before surgical induction, 4 weeks, 8 weeks, and 12 weeks after surgery. Briefly, mice were run on a transparent conveyor belt at a fixed speed (18 cm/sec) while images were acquired with a high-speed camera from the abdomen. Animals ran for a maximum of 20 seconds per measurement, and 5-second segments (over 10 consecutive strides) were selected for analysis. Animals stopped on the track or ran back and forth as failed experiments. Meanwhile, the paw swing time, standing time, and contact area were used as reference items for previously reported models of intervertebral disc injury and paravertebral muscles for gait analysis.<sup>28,29</sup>

## In vivo Fluorescence Imaging

First, the NF- $\kappa$ B Luciferase reporter mice were anesthetized with isoflurane, and then the luminescent agent D-luciferin (1.5 mg/10 g) dissolved in normal saline was injected intraperitoneally. According to previous studies, the peak taste signal is 10 minutes after D-luciferin injection.<sup>10,26</sup> Whole body images were acquired using Living Image Software (Andor Newton, DZ436) with an exposure time of approximately 10 seconds. Three 10-week-old male mice per group.

## Micro-Computed Tomography ( $\mu$ CT) Analysis

The spinal tissues from the thirteenth thoracic vertebra to the first sacral vertebra were collected from 12-week-old mice, and the muscle tissue around the spine was peeled off and fixed in 4% cell tissue fixative for three days. The fixed tissue samples were placed in the  $\mu$ CT mice bed along the sagittal direction for X-ray scanning. The scanning parameters are as follows: the scanning software SkyScan1176, the resolution is 8.73  $\mu$ m, the voltage is 42 kV, the current is 555  $\mu$ A, the exposure time is 786 ms, the filter is Al 0.2 mm, the spiral scan is 180°, and 2 images are captured every 0.3° on average. After scanning, the airborne NRecon reconstruction software and CTvox graphics software were used for 3D reconstruction and 3D image establishment to observe the size of lumbar intervertebral disc tissue and the formation of endplate ossification. Finally, the Region of Interest (ROI) was quantitatively analyzed using the airborne bone micro morphometric analysis software CTAn.<sup>26</sup>

## Histomorphological Staining

After fixation, the samples were washed with running water and the residual fixative on the surface was immersed in 14% EDTA solution for decalcification for 14 days. Then, the surface was washed with running water to decalcify and then put into graded alcohol for dehydration and subsequent paraffin embedding. The paraffin tissue was stained in 3  $\mu$ m thick sections. After the sections were deparaffinized and rehydrated, Alcian Blue/Hematoxylin & Orange G staining (ABH staining) was used to observe the morphology of the lumbar intervertebral disc tissue. According to the ABH staining results and the histological evaluation scale of lumbar intervertebral disc tissue, the data of each histological variable in the structure of the IVD and cartilage endplate were evaluated respectively.<sup>30</sup>

## Immunohistochemical Staining (IHC)

For IHC detection, sections were treated with 0.01 M citrate buffer (Solarbio, Beijing, China) at 60 °C for 4 h after completion of deparaffinization and rehydration as antigen retrieval. Next, sections were incubated in Col2, Mmp-13, TNF- $\alpha$ , and p-P65 primary antibodies overnight at 4°C. After incubation with the homologous secondary antibody for 20 minutes on the next day, positive staining was detected with diaminobenzidine (DAB) solution and counterstained with hematoxylin. Positive staining was assessed semi-quantitatively using Image-Pro Plus software (Media Cybernetics, Silver Spring, USA).

## Cell Culture

Primary chondrocytes were obtained from two-week-old C57BL/6J mice. The mice were sacrificed and sterilized by immersion in 75% alcohol, and the lumbar endplate cartilage was aseptically isolated. Then, the tissue was washed three times with phosphate-buffered saline, transferred to DMEM/F12 medium containing 0.25% collagenase, and digested overnight in a cell incubator. The next day, the digested primary chondrocytes were cultured in DMEM/F12 medium containing 10% FBS and 1% streptomycin/penicillin, and incubated at 37°C and 5% CO<sub>2</sub> in an incubator for subsequent experiments.

## Quantitative Real-Time PCR (qPCR) Detection

The primary chondrocytes cultured in vitro were added with 500 µL Trizol solution, and RNA was extracted and reverse transcribed according to the operating instructions of RNeasy Mini Kit (QIAGEN) and All-in-One cDNA Synthesis SuperMix (Bimake). Then, qPCR detection was performed with 2x SYBR Green qPCR Master Mix (Low ROX) (Bimake) reagent. Quantitative analysis was performed using β-actin as a control gene. Table 1 showed the primer sequences of target genes used in the current study.

## Western Blot

Add an appropriate amount of RIPA lysis solution (containing protease inhibitors, currently used) to the primary chondrocytes cultured in vitro. After repeated shaking on ice for 30 minutes, centrifuge at 12,000 rpm for 10 minutes at 4°C, and aspirate the supernatant into a new 1.5mL centrifuge tube. First, use a BCA protein quantification kit to measure the protein concentration of each histone, then add a certain volume of 5× loading buffer to the remaining protein supernatant (to make the final concentration 1×), and boil for 15 min at 100°C for denaturation. Then, proteins (20 µg/lane) were separated by 8% SDS-PAGE gel and transferred to the PVDF membrane. After 1-hour incubation with 5% skim milk, IKBα (1:1000 dilution, HuaBio), p-IKBα (1:1000 dilution, HuaBio), P65 (1:1000 dilution, Cell Signaling Technology), p-P65 (1:1000 dilution, Cell Signaling Technology), and β-actin (1:10,000 dilution, Sigma-Aldrich) and other primary antibodies were incubated at 4°C for 12 hours. Afterward, it was incubated with the corresponding homologous secondary antibody for 1 hour at room temperature, and finally, the visualization of protein bands was performed with Image Quant LAS 4000 (EG, United States). Using β-actin as an internal reference, the gray value of the protein band was calculated by Image-Pro Plus 6.0 software, and the expression of the target protein among each group was analyzed.

## Statistical Analysis

All experimental data of this subject were analyzed by GraphPad Prism software version 8.0, and the statistical results of measurement data were expressed as mean ± standard deviation. One-way analysis of variance (One-way ANOVA) was

**Table 1** Primer Sequences for Quantitative RT-PCR

Primer Name	Primer Sequence (5'→3')
<i>Aggrecan</i> Forward	CAGTGCGATGCAGGCTGGCT
<i>Aggrecan</i> Reverse	CCTCCGGCACTCGTTGGCTG
<i>TNFα</i> Forward	CCCTCACACTCAGATCATCTTCT
<i>TNFα</i> Reverse	GCTACGACGTGGGCTACAG
<i>Mmp-13</i> Forward	TTTGAGAACACGGGGAAGA
<i>Mmp-13</i> Reverse	ACTTTGTTGCCAATTCCAGG
<i>Col2</i> Forward	TGGTCCTCT GGGCATCTCAGGC
<i>Col2</i> Reverse	GGTGAACCTGCTGTTGCCCTCA
<i>β-actin</i> Forward	GGAGATTACTGCCCTGGCTCCTA
<i>β-actin</i> Reverse	GACTCATCGTACTCCTGCTTGCTG



used for comparison between different groups, and Dunnett's T3 test was used if the variance was not homogeneous. The difference was statistically significant with  $P < 0.05$ .

## Results

### AMD Alleviates LSI Surgery-Induced NF- $\kappa$ B Activity and Pain

Previous studies have shown that AMD plays an important role in anti-inflammation, while NF- $\kappa$ B activity is associated with inflammation in IDD (Figure 1A). Therefore, we used NF- $\kappa$ B Luciferase reporter mice to detect AMD in the early stage of IDD anti-inflammatory effect. In this study, we used the LSI mouse model to simulate the progression of IDD. Subsequently, luminescence observation was performed on the 14th postoperative day, and the images showed that the NF- $\kappa$ B activity of the lumbar spine in the surgical area was significantly higher than that of other parts of the spine, and more importantly, AMD treatment significantly inhibited the NF- $\kappa$ B activity in the LSI surgical area. Then, quantitative analysis showed that high-dose (0.5 mg/kg) AMD treatment reduced NF- $\kappa$ B activity by about half compared with the normal saline group, while NF- $\kappa$ B activity was almost completely after low-dose (0.1 mg/kg) AMD treatment disappeared, suggesting that the anti-inflammatory effect of AMD may be counteracted by its toxicological effects with increasing dose (Figure 1B and C). Based on the above experiments, we performed subsequent *in vivo* experiments using an AMD dose of 0.1 mg/kg. Taken together, these results suggest that AMD can inhibit LSI surgery-induced NF- $\kappa$ B activity and possibly suppress the inflammatory response during IDD progression.

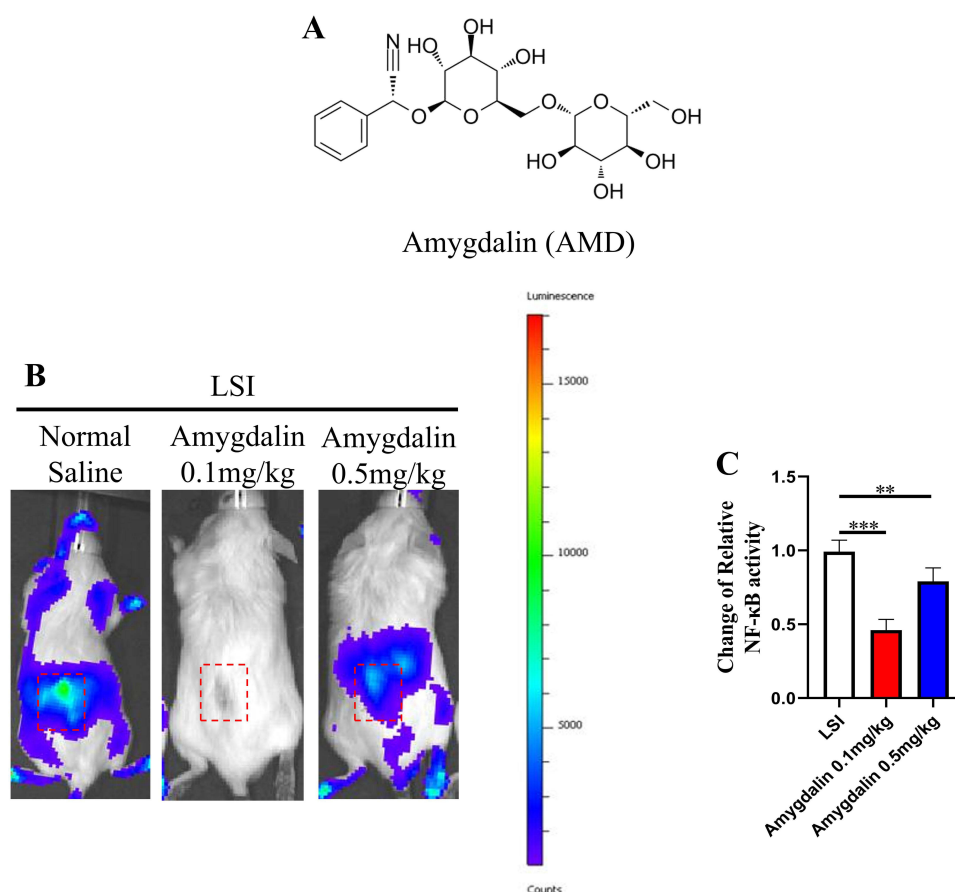


**Figure 1** AMD suppressed NF- $\kappa$ B activity at low back in LSI mice. **(A)** The chemical structure of Amygdalin. **(B)** Representative images of NF- $\kappa$ B luciferase activity at days 14 after operation. Red dashed box indicated ROI for assessments. **(C)** Quantitative analysis of relative-change of NF- $\kappa$ B activity in ROI. Data were presented as means  $\pm$  S.D. \*\* $p < 0.01$ ; \*\*\* $p < 0.001$ ,  $n = 3$  in each group.

## AMD Delays Gait Abnormalities in LSI Surgery-Induced IDD Mice Model

Discogenic low back pain is one of the causes of non-specific LBP, and non-specific LBP is one of the major problems associated with bipedal walking.<sup>31,32</sup> Previous studies have also reported changes in mouse gait behavior in a model of IDD.<sup>29</sup> Therefore, Gait was used to determine whether AMD could alleviate LBP caused by LSI surgery-induced IDD (Figure 2A and B). As shown in Figure 2C and E, LSI surgery induced an increase in standing time and paw contact area and a decrease in swing time in mice compared with the sham-operated group. AMD treatment significantly increased swing time and decreased standing time and contact area in IDD model mice. These results suggest that AMD can improve discogenic low back pain and alleviate gait impairment caused by LSI.

## AMD Attenuates LSI-Induced Disc Degeneration and Endplate Porosity

Loss of disc height is one of the typical features of IDD, and we first observed the spatial changes in the lumbar intervertebral space. The coronal lumbar spine scan images showed that the LSI procedure resulted in a significant narrowing of the intervertebral space between L4-L5. Interestingly, LSI-induced intervertebral space stenosis could be ameliorated after AMD treatment (Figure 3A and B). In addition, we performed 3D reconstruction of the IVD and cartilaginous endplates, and consistent with the trend of intervertebral space size changes, AMD treatment prevented LSI surgery-induced reduction of L4-L5 intervertebral disc height (Figure 3C). At the same time, the 3D reconstruction map also showed that the cavity in the ossified area of the endplate was the main reason for the reduction of the volume of the IVD, while the cartilage endplate of the sham-operated mice remained relatively intact. Importantly, the porosity of the cartilage endplates of mice after 8 weeks of AMD treatment was significantly reduced compared with the model group (Figure 3D). These data suggest that AMD can ameliorate the progression of LSI surgery-induced IDD.

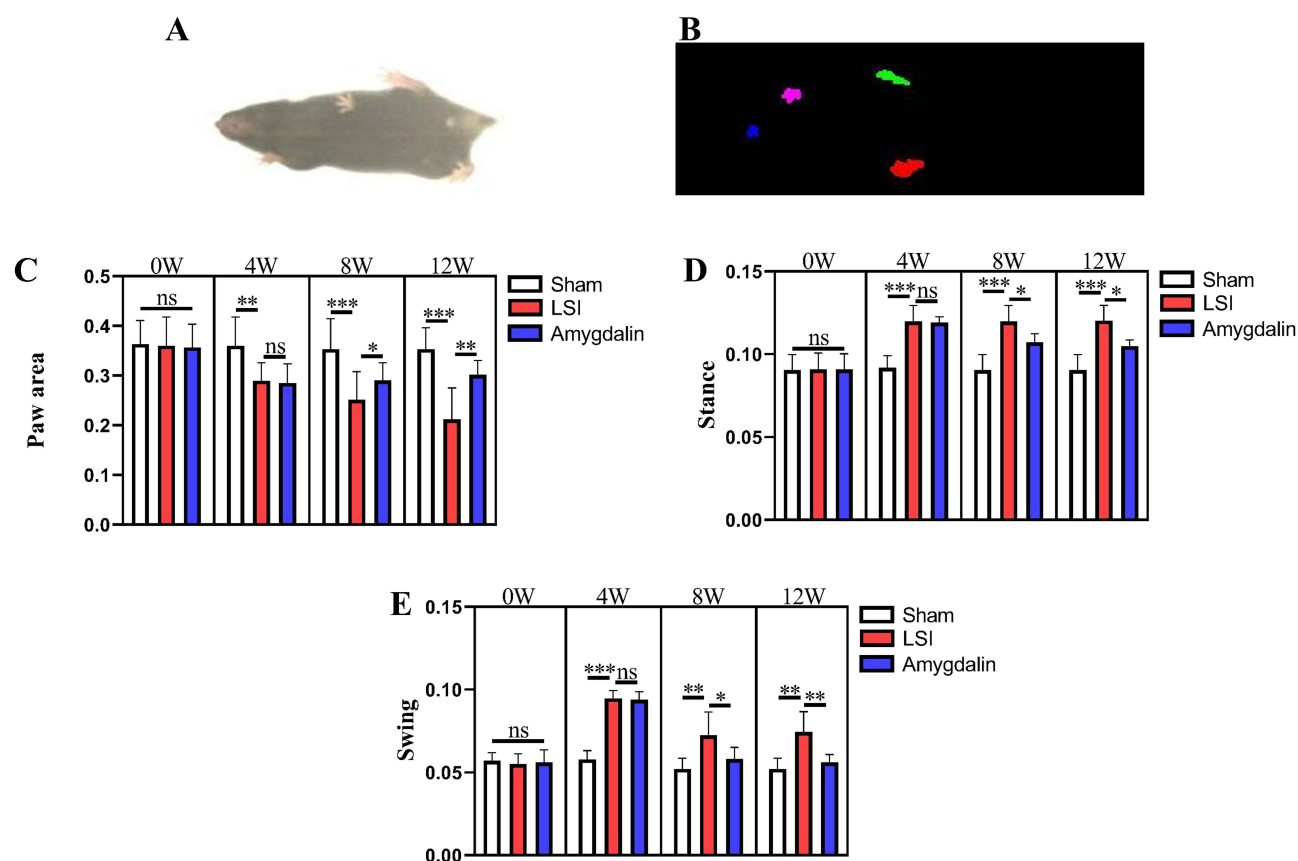


**Figure 2** AMD alleviates gait impairment in LSI mice. (A) Top view of mouse gait; (B) trajectory diagram of mouse paws; (C–E) statistical analysis of swing time, standing time, and paw basking area in mice 0, 4, 8, and 12 weeks after LSI surgery gait analysis, respectively. Data were presented as means  $\pm$  S.D. \* $P < 0.05$ ; \*\* $P < 0.01$ ; \*\*\* $P < 0.001$ ; ns, significant difference,  $n = 6$  in each group.

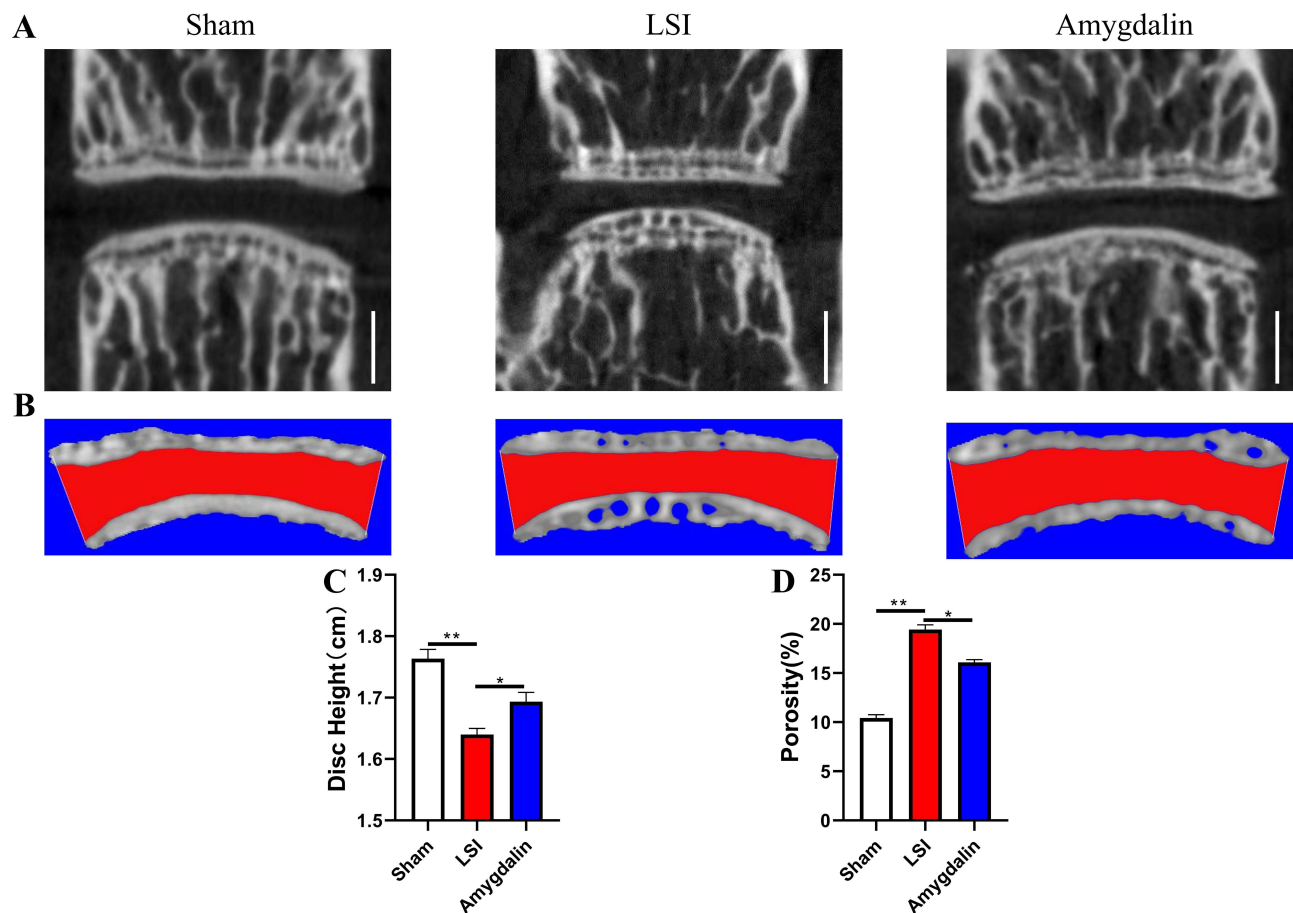


**Figure 3** AMD mitigated intervertebral disc degeneration in LSI mice. **(A)** Representative micro-CT images of a midsagittal plane at L4-L5. **(B)** Representative 3D-reconstruction images of L4-L5 endplate with the coronal plane. The red area indicated IVD space. **(C)** Quantitative analysis of disc height at L4-L5. **(D)** Quantitative analysis of the endplate porosity at L4-L5. Data were presented as means  $\pm$  S.D. \* $P < 0.05$ ; \*\* $P < 0.01$ ,  $n = 6$  in each group.

## AMD Protects Against LSI-Induced Cartilage Endplate Calcification and Degeneration

The radiographic findings have suggested that AMD can improve IDD. We next explored the effect of AMD on cartilage endplates using ABH staining to assess the degree of endplate degeneration. Compared with the mice in the sham group, the mice in the model group had severe cartilage matrix loss, obvious endplate calcification, and increased bone marrow cavity 12 weeks after surgery (Figure 4A). Consistent with the  $\mu$ CT results, AMD treatment significantly improved LSI surgery-induced cartilage endplate calcification and degeneration (Figure 4A). Meanwhile, the IVD and endplate scores of the AMD treatment group were significantly lower than those of the model group (Figure 4B and C). For changes in endplate thickness, we found that AMD treatment did not delay an LSI-induced increase in the thickness of cartilage endplates (Figure 4D and E). Likewise, the endplate thickness of the sham-operated group was not statistically different from that of the model group (Figure 4D and E). This may be due to slight changes in IVD with age. In a pooled analysis of the above data, AMD treatment protected the degeneration of cartilage endplates in the LSI surgical model.

## AMD Delays LSI Surgery-Induced Degradation of Cartilage Matrix

ECM is an important tissue structure for the IVD to bear the pressure load, and CEP, as an important structural component of the IVD, can not only relieve and disperse the axial pressure on the NP but also the way of transporting nutrients in the internal tissue of the IVD. Given that AMD can alleviate the degeneration of cartilage endplates in mice after LSI surgery, we further confirmed whether it affects the metabolism of the cartilage matrix in IDD progression. Col2 is the main component of ECM and CEP cells. The expression of Mmp-13 directly determines the degree of Col2 degradation. The expression levels of the two can indirectly indicate the degradation of ECM and CEP. Using IHC to

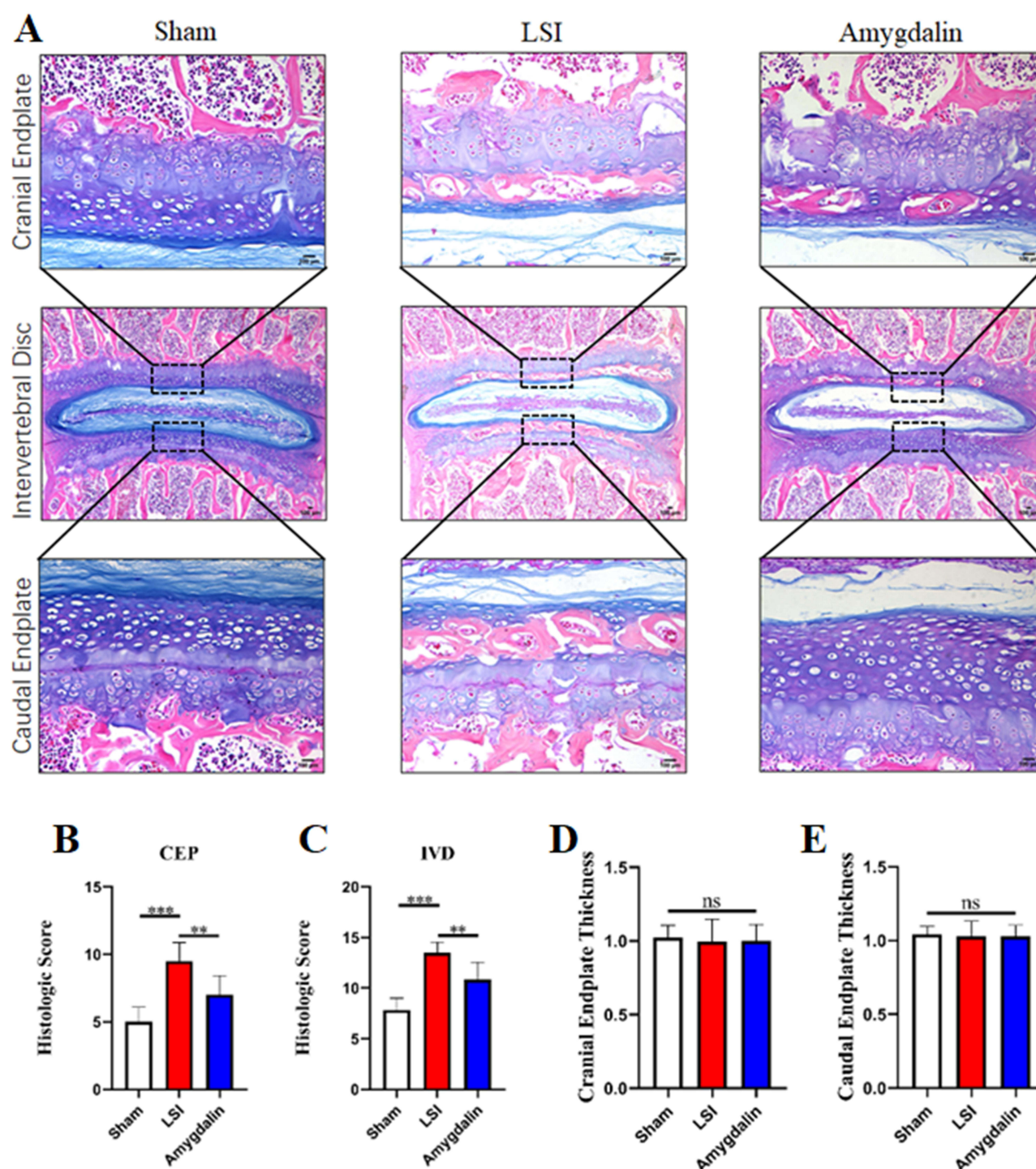


**Figure 4** AMD attenuated cartilaginous endplate calcification in LSI mice. **(A)** Alcian Blue Hematoxylin/Orange G staining of cranial L4–L5 endplate (top panels, high magnification), caudal L4–L5 endplate (bottom panels, high magnification), and the whole L4–L5 IVD (middle panels, low magnification) at 12 weeks after operations. **(B and C)** Quantitative analysis of L4–L5 endplate score and IVD score at 12 weeks post-operation. **(D and E)** Quantitative analyses of cranial or caudal L4–L5 endplate thickness. Data were presented as means  $\pm$  S.D.  $**P < 0.01$ ;  $***P < 0.001$ ; ns: significant difference,  $n = 6$  in each group.

detect its spatial expression, the results showed that the expression of Col2 in the IVD tissue of the mice in the model group was significantly reduced, and the expression of Mmp-13 was significantly increased (Figure 5A–D). On the contrary, AMD intervention could significantly inhibit the down-regulation of Col2 expression and the increase of Mmp-



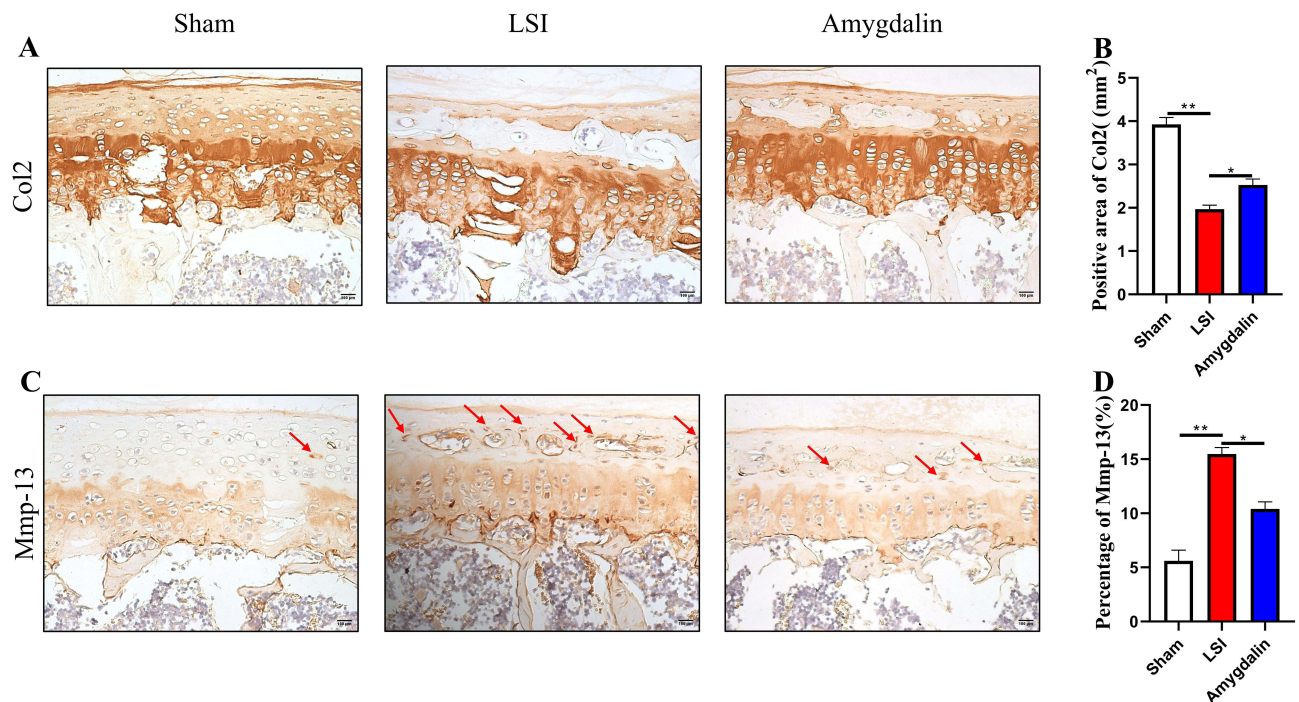


**Figure 5** The effect of AMD on LSI-induced anabolism and catabolism in cartilage endplate. **(A)** The representative images of immunohistochemical staining of Col2 in the caudal L4–L5 endplate at 12 weeks. **(B)** Immunostaining images evaluation of Mmp-13 expression in caudal L4–L5 endplate at 12 weeks post-operation. Red arrows indicated positive cells. **(C and D)** Quantitative analyses of the rate of positive areas. Data were presented as means  $\pm$  S.D. \* $P < 0.05$ ; \*\* $P < 0.01$ ,  $n \geq 4$  in each group.

13 expression in the IVD tissue of mice (Figure 5A–D). These data provide new insights into the anti-degradation of cartilage matrix in AMD to delay IDD.

## AMD Inhibits the Expression of Inflammatory Factors and the Activation of NF- $\kappa$ B Signaling Pathway in the Endplate of IDD

The intervention of inflammatory cytokines is one of the main factors leading to the degenerative changes of the IVD and the normal metabolic imbalance of the IVD. Moreover, studies have found that inflammatory cytokines can accelerate the decomposition of ECM, and TNF- $\alpha$  is closely related to IDD.<sup>33</sup> Therefore, we next examined its expression by IHC. As expected, AMD suppressed LSI manipulation-induced elevation of TNF- $\alpha$  (Figure 6A and B). In addition, there is also a close relationship between TNF- $\alpha$  and NF- $\kappa$ B signaling pathways.<sup>34,35</sup> Although we reported increased NF- $\kappa$ B activity in the lumbar dorsum after LSI surgery by NF- $\kappa$ B Luciferase reporter mice and significantly attenuated its activity by AMD (0.1 mg/kg) treatment, whether AMD could inhibit NF- $\kappa$ B activity in endplate chondrocytes NF- $\kappa$ B signaling is not well defined. Therefore, we examined the phosphorylation levels of P65 using IHC to assess the AMD response to NF- $\kappa$ B signaling. It was found that AMD significantly inhibited LSI-induced phosphorylation of P65 in endplate chondrocytes in IDD (Figure 6C and D). These data suggest that AMD-delayed IDD progression is closely related to the inhibition of NF- $\kappa$ B signaling pathway activation and inflammatory factor secretion.

## AMD Abolished the Activation, Catabolism, and Inflammation of NF- $\kappa$ B Signaling Pathway in Chondrocytes Induced by IL-1 $\beta$ Treatment in vitro

The above data suggest that AMD can alleviate the degeneration of endplate chondrocytes in vivo. Therefore, we used primary chondrocytes to investigate the effect of AMD on IL-1 $\beta$  treatment of primary chondrocytes in vitro. First, we performed qRT-PCR assays, and the data showed that AMD significantly decreased the mRNA expression of Mmp-13 and TNF- $\alpha$ , while increasing the expression levels of Col2 and Aggrecan genes, which was consistent with the trend of in vivo IHC results (Figure 7A–D). Then, the changes of these protein expression levels of p-P65 and p-IK $\beta$ , the key



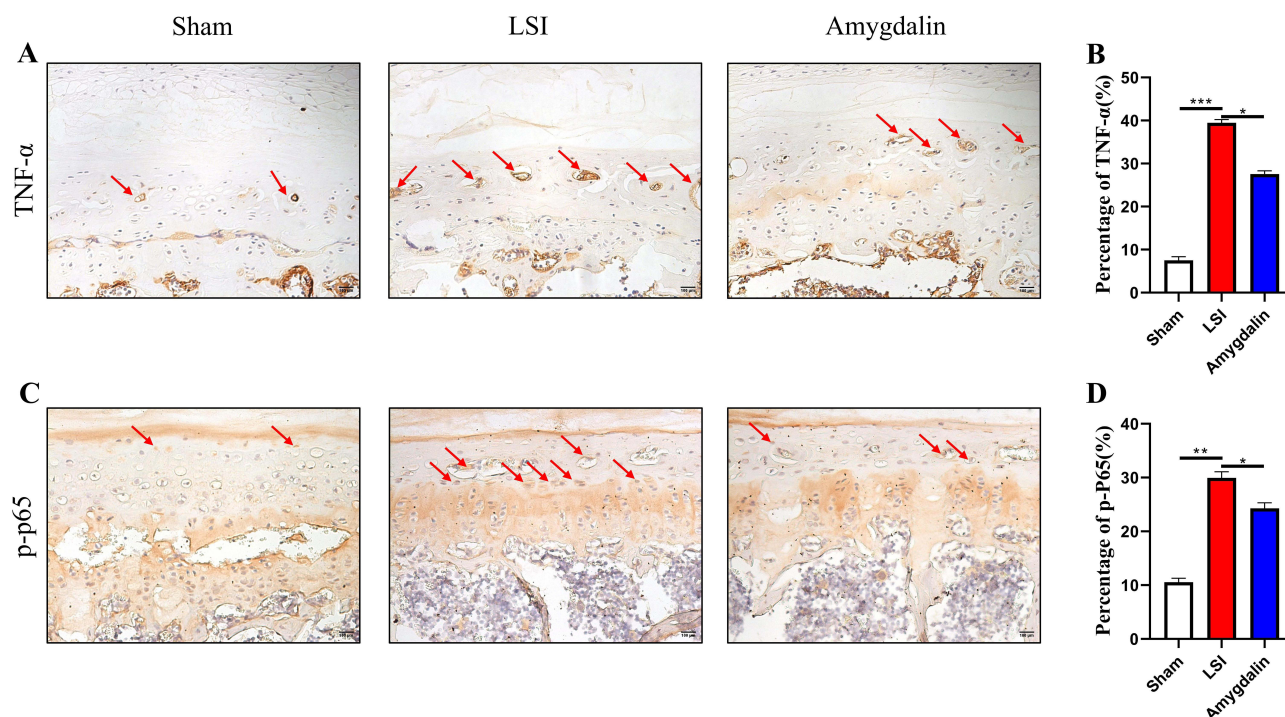


**Figure 6** AMD repressed LSI-induced activation of NF- $\kappa$ B signaling in endplate chondrocytes. **(A and B)** The representative images of immunohistochemical staining and quantifications of TNF- $\alpha$  in the caudal L4–L5 endplate at 12 weeks. Red arrows indicated positive cells. **(C and D)** The representative images of immunohistochemical staining and quantifications of phosphorylated-P65 in the caudal L4–L5 endplate at 12 weeks. Red arrows indicated positive cells. Data were presented as means  $\pm$  S.D. \* $P$  < 0.05; \*\* $P$  < 0.01; \*\*\* $P$  < 0.001,  $n \geq 4$  in each group.

factor in the NF- $\kappa$ B signaling pathway, were determined by Western blot. The data showed that these proteins' expression levels of p-P65 and p-IKB $\alpha$  were significantly increased in IL-1 $\beta$ -treated chondrocytes, while AMD could inhibit the high expression of p-P65 and p-IKB $\alpha$ , showing a similar effect to BAY11-7082 (Figure 7E–G). These above experimental data validate the in vivo experiments showing that AMD partially inhibits the activation of NF- $\kappa$ B signaling pathway to protect chondrocytes from catabolism and inflammation.

## Discussion

LBP is one of the most common symptoms in the human musculoskeletal system. Lumbar intervertebral disc degeneration is one of the most common causes of LBP, and the degree of LBP is closely related to the degree of IDD.<sup>36,37</sup> There are many current treatments for LBP and IDD, but most of them only relieve the patient's symptoms, and have no therapeutic effect on the underlying disease of IVD.<sup>38,39</sup> In the present study, our results showed that AMD delayed ECM degradation and release of inflammatory factors, and calcification of cartilage endplates during IDD by partially inhibiting the activation of NF- $\kappa$ B signaling pathway. Therefore, these findings suggest that AMD may serve as a potential treatment for IDD.

A good animal model is one of the important guarantees for scientific research, which can provide an effective observational basis for understanding the pathophysiological changes of diseases and drug efficacy. In the present study, we simulated the progression of IDD using an LSI mouse model consistent with the radiological and histological features of human IDD.<sup>40</sup> Previous studies have found reduced disc volume and altered endplate calcification in LSI-operated mice.<sup>26,41</sup> Likewise, our data show that the thickening of cartilage endplate calcification in a mouse model of LSI surgery is positively associated with a reduction in disc volume, which is consistent with previous studies in mice.<sup>40</sup> In addition, based on  $\mu$ CT and ABH staining in the current study, we found that AMD treatment was able to alleviate these structural changes induced by LSI surgery, thereby delaying the progression of IDD.

IVD is a complex tissue. Previous studies have mainly focused on the nucleus pulposus and annulus fibrosus, while changes in the cartilage endplate are rarely reported. With the in-depth study of the entire tissue of the intervertebral disc,

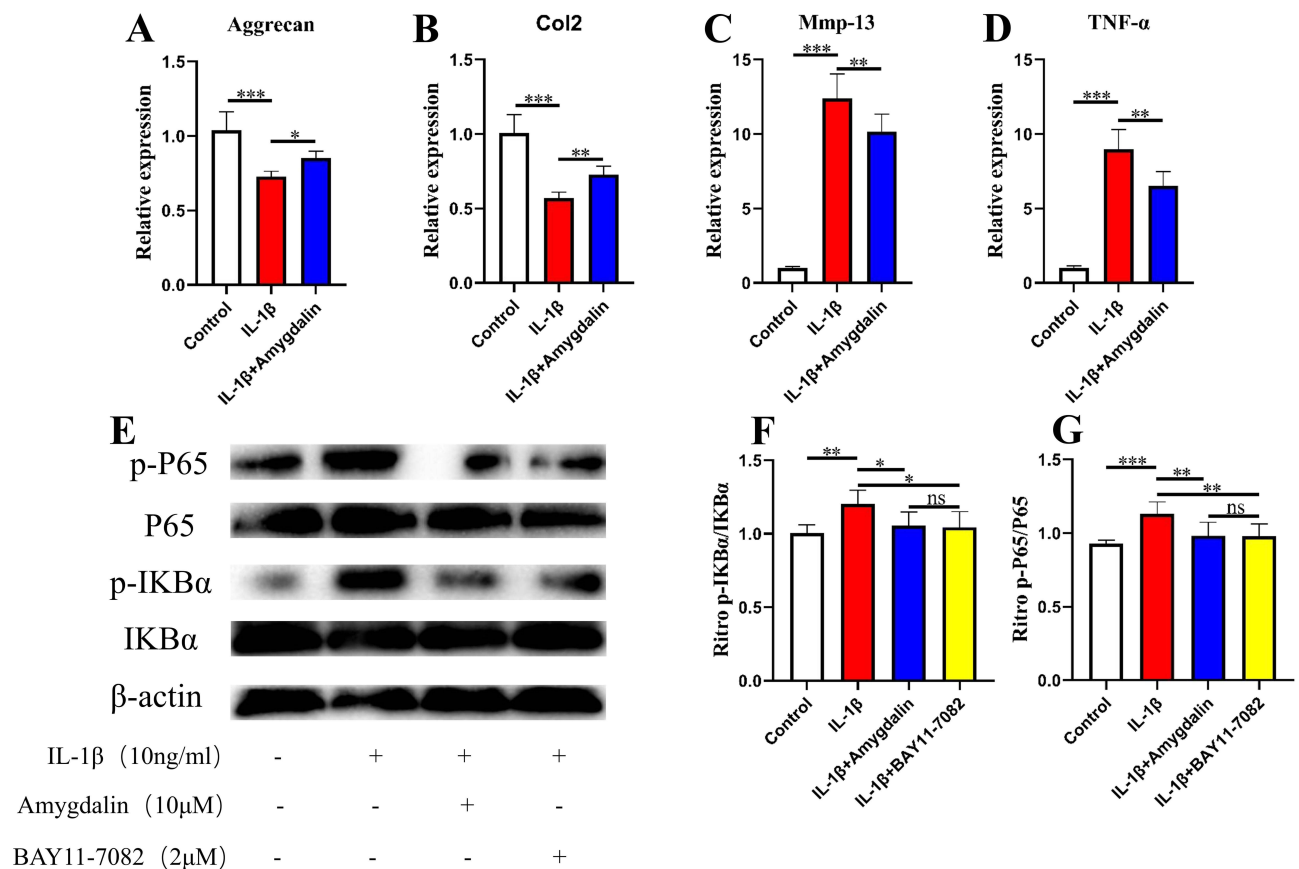


**Figure 7** The effect of AMD on IL-1 $\beta$ -induced chondrocytes in vitro. (A–D) The gene expression of IL-1 $\beta$ -induced chondrocytes was treated with various concentrations of AMD for 24 h. (E–G) The NF- $\kappa$ B signaling pathway-related proteins expression of IL-1 $\beta$ -induced chondrocytes treated with various concentrations of AMD and NF- $\kappa$ B inhibitor (BAY 11-7082) for 24 h. Data were presented as means  $\pm$  S.D. \* $P$  < 0.05; \*\* $P$  < 0.01; \*\*\* $P$  < 0.001; ns, significant difference,  $n$  = 3 in each group.

cartilage endplate deformation has also been identified as a key factor in the pathogenesis of IDD.<sup>42</sup> The cartilage endplate of the vertebral body is the main nutritional pathway of IVD, which plays a role in the nutritional supply and maintenance of the mechanical properties of IVD. Obstruction of the nutritional pathway of the endplate can lead to the occurrence of IDD.<sup>43</sup> In the present study, ABH staining results showed that cartilage endplates were significantly calcified and thickened and increased porosity at 12 weeks of LSI surgery. But AMD treatment reversed these changes, suggesting that AMD can inhibit endplate calcification and slow the progression of IDD. In addition, CEP cells are chondrocytes embedded in the hyaline cartilage matrix. The mechanical function of the IVD is controlled by the extracellular matrix, which is mainly composed of two major macromolecules, collagen and proteoglycans, and maintaining the integrity of the extracellular matrix is essential for a healthy, normal IVD.<sup>44</sup> Col2 is the main component of ECM and CEP cells. The expression of Mmp-13 directly determines the degree of Col2 degradation. The expression levels of the two can indirectly indicate the degradation of ECM and CEP. In the present study, the expression of Col2 was increased and Mmp-13 was down-regulated in the cartilage endplates of AMD-treated mice compared with mice in the model group. Therefore, the therapeutic effect of AMD can be explained in part by inhibiting the imbalance of extracellular matrix metabolism to maintain the properties of cartilage endplates, thereby delaying endplate calcification and degeneration.

ECM degradation and inflammatory factors are known as hallmarks of IDD, and they are interrelated and interdependent. Pro-inflammatory cytokines lead to the dysregulation of ECM metabolism by up-regulating the expression of ECM-degrading enzymes and down-regulating ECM structural components.<sup>45</sup> Intrinsic degradation of the ECM leads to extracellular accumulation of ECM fragments that further stimulate the inflammatory response.<sup>46</sup> Meanwhile, inflammatory cytokines and metalloproteinases are the two most important regulators in

IDD and are closely related to NF- $\kappa$ B signaling.<sup>47</sup> Based on previous studies, we used luciferase reporter mice to detect NF- $\kappa$ B activity in vivo.<sup>10</sup> Our results are consistent with previous studies, confirming that both the LSI surgery model and other IDD models can induce an increase in the activity of NF- $\kappa$ B.<sup>48</sup> In addition, previous studies have shown that inflammatory factors (such as IL-1 $\beta$  and TNF- $\alpha$ ) are closely related to the NF- $\kappa$ B signaling pathway and are closely related to IDD.<sup>34,35</sup> In the present study, AMD significantly inhibited the activation of NF- $\kappa$ B signaling pathway and the expression of inflammatory factor (TNF- $\alpha$ ) induced by LSI surgery. It indicated that AMD may lead to the progression of IDD by inhibiting the NF- $\kappa$ B signaling pathway induced by inflammatory factors. In addition, in vitro experiments on chondrocytes treated with AMD and NF- $\kappa$ B inhibitors showed that the gene and protein expressions of Mmp-13, IL-1 $\beta$ , and TNF- $\alpha$  were similar, indicating that AMD may act as an inhibitor of NF- $\kappa$ B signaling pathway, while suppressing inflammation. The release of factors, thereby delaying the IDD process.

Studies have shown that many traditional herbal medicines and their active ingredients have anti-inflammatory properties and are potential treatments for IDD.<sup>10,49,50</sup> The anti-inflammatory effects of AMD in various diseases have been extensively studied as follows: Liver damage, lung damage, osteoarthritis, and asthma.<sup>21,24,51,52</sup> Meantime, AMD could inhibit the degeneration of the endplate chondrocytes derived from intervertebral discs of rats induced by IL-1 $\beta$ .<sup>29</sup> This study confirmed that AMD slowed the progression of IDD by reducing the inflammatory response. In addition, pain is the result of inflammation, and analgesic effects have also been reported in AMD.<sup>20,53</sup> These data suggest that AMD may relieve pain symptoms and slow disease progression in IDD by inhibiting the inflammatory response.

The current study has several limitations. First, we only used small animal models to study AMD therapeutic effects of IDD, the effect of AMD on large animals needs to be further investigated. Second, AMD has a strong toxicological effect. How to avoid and detect its damage to animal bodies. We will continue to study these contents deeply in the future.

## Conclusions

In conclusion, this study elucidates that AMD alleviates pain symptoms and progression of IDD by partially inhibiting NF- $\kappa$ B signaling, preventing inflammatory factors, catabolism, endplate calcification, and endplate chondrocyte degeneration. The course of the disease. Therefore, our study suggests that AMD may be a potential alternative therapy for IDD.

## Data Sharing Statement

The data used to provide support for the results of this study can be obtained from the corresponding authors.

## Acknowledgments

We appreciate the great help from the Public Platform of Medical Research Center, Academy of Chinese Medical Science, Zhejiang Chinese Medical University.

## Author Contributions

All authors made a significant contribution to the work reported, whether that is in the conception, study design, execution, acquisition of data, analysis and interpretation, or in all these areas; took part in drafting, revising or critically reviewing the article; gave final approval of the version to be published; have agreed on the journal to which the article has been submitted; and agree to be accountable for all aspects of the work.

## Funding

This research has been partially supported by the Natural Science Foundation of China (Grant nos. 82274549), the Natural Science Foundation of Zhejiang Province (LY23H27005), the State Administration of Traditional Chinese Medicine of Zhejiang Province (2022ZB116).

## Disclosure

All authors declare that they have no conflicts of interest.

## References

- Amorim AB, Simic M, Pappas E, et al. Is occupational or leisure physical activity associated with low back pain? Insights from a cross-sectional study of 1059 participants. *Braz J Phys Ther*. 2019;23(3):257–265. doi:10.1016/j.bjpt.2018.06.004
- Stanislawska I, Mincewicz M, Cabak A, et al. Epidemiological aspects of low back pain. *Adv Exp Med Biol*. 2019;1176:47–52.
- Kennon JC, Awad ME, Chutkan N, DeVine J, Fulzele S. Current insights on use of growth factors as therapy for intervertebral disc degeneration. *Biomol Concepts*. 2018;9(1):43–52. doi:10.1515/bmc-2018-0003
- Vadala G, Russo F, Di Martino A, Denaro V. Intervertebral disc regeneration: from the degenerative cascade to molecular therapy and tissue engineering. *J Tissue Eng Regen Med*. 2015;9(6):679–690. doi:10.1002/term.1719
- The L. GBD 2017: a fragile world. *Lancet*. 2018;392(10159):1683. doi:10.1016/S0140-6736(18)32858-7
- Yan Z, Pan Y, Wang S, et al. Static compression induces ECM remodeling and Integrin alpha2beta1 expression and signaling in a rat tail caudal intervertebral disc degeneration model. *Spine*. 2017;42(8):E448–E458. doi:10.1097/BRS.0000000000001856
- Newell N, Little JP, Christou A, Adams MA, Adam CJ, Masouros SD. Biomechanics of the human intervertebral disc: a review of testing techniques and results. *J Mech Behav Biomed Mater*. 2017;69:420–434. doi:10.1016/j.jmbbm.2017.01.037
- Nguyen QT, Jacobsen TD, Chahine NO. Effects of inflammation on multiscale biomechanical properties of cartilaginous cells and tissues. *ACS Biomater Sci Eng*. 2017;3(11):2644–2656. doi:10.1021/acsbomaterials.6b00671
- Wu X, Li S, Wang K, et al. TNF-alpha regulates ITGBeta1 and SYND4 expression in nucleus pulposus cells: activation of FAK/PI3K signaling. *Inflammation*. 2019;42(5):1575–1584. doi:10.1007/s10753-019-01019-9
- Ge Q, Ying J, Shi Z, et al. Chlorogenic Acid retards cartilaginous endplate degeneration and ameliorates intervertebral disc degeneration via suppressing NF-kappaB signaling. *Life Sci*. 2021;274:119324.
- Sun J, Hong J, Sun S, et al. Transcription factor 7-like 2 controls matrix degradation through nuclear factor kappaB signaling and is repressed by microRNA-155 in nucleus pulposus cells. *Biomed Pharmacother*. 2018;108:646–655. doi:10.1016/j.biopha.2018.09.076
- Wang S, Li J, Tian J, et al. High amplitude and low frequency cyclic mechanical strain promotes degeneration of human nucleus pulposus cells via the NF-kappaB p65 pathway. *J Cell Physiol*. 2018;233(9):7206–7216. doi:10.1002/jcp.26551
- Cazzanelli P, Wuertz-Kozak K. MicroRNAs in intervertebral disc degeneration, apoptosis, inflammation, and mechanobiology. *Int J Mol Sci*. 2020;21(10):3601. doi:10.3390/ijms21103601
- Wang Y, Che M, Xin J, Zheng Z, Li J, Zhang S. The role of IL-1beta and TNF-alpha in intervertebral disc degeneration. *Biomed Pharmacother*. 2020;131:110660. doi:10.1016/j.biopha.2020.110660
- Zhang GZ, Liu MQ, Chen HW, et al. NF-kappaB signalling pathways in nucleus pulposus cell function and intervertebral disc degeneration. *Cell Prolif*. 2021;54(7):e13057. doi:10.1111/cpr.13057
- Li Z, Wang X, Pan H, et al. Resistin promotes CCL4 expression through toll-like receptor-4 and activation of the p38-MAPK and NF-kappaB signaling pathways: implications for intervertebral disc degeneration. *Osteoarthritis Cartilage*. 2017;25(2):341–350. doi:10.1016/j.joca.2016.10.002
- Guo J, Wu W, Sheng M, Yang S, Tan J. Amygdalin inhibits renal fibrosis in chronic kidney disease. *Mol Med Rep*. 2013;7(5):1453–1457. doi:10.3892/mmr.2013.1391
- Jaswal V, Palanivelu J, R C. Effects of the Gut microbiota on Amygdalin and its use as an anti-cancer therapy: substantial review on the key components involved in altering dose efficacy and toxicity. *Biochem Biophys Rep*. 2018;14:125–132. doi:10.1016/j.bbrep.2018.04.008
- Baroni A, Paoletti I, Greco R, et al. Immunomodulatory effects of a set of amygdalin analogues on human keratinocyte cells. *Exp Dermatol*. 2005;14(11):854–859. doi:10.1111/j.1600-0625.2005.00368.x
- Hwang HJ, Kim P, Kim CJ, et al. Antinociceptive effect of amygdalin isolated from *Prunus armeniaca* on formalin-induced pain in rats. *Biol Pharm Bull*. 2008;31(8):1559–1564. doi:10.1248/bpb.31.1559
- Hwang HJ, Lee HJ, Kim CJ, Shim I, Hahm DH. Inhibitory effect of amygdalin on lipopolysaccharide-inducible TNF-alpha and IL-1beta mRNA expression and carrageenan-induced rat arthritis. *J Microbiol Biotechnol*. 2008;18(10):1641–1647.
- Zhang X, Hu J, Zhuo Y, et al. Amygdalin improves microcirculatory disturbance and attenuates pancreatic fibrosis by regulating the expression of endothelin-1 and calcitonin gene-related peptide in rats. *J Chin Med Assoc*. 2018;81(5):437–443. doi:10.1016/j.jcma.2017.09.005
- Kung YL, Lu CY, Badrealam KF, et al. Cardioprotective potential of amygdalin against angiotensin II induced cardiac hypertrophy, oxidative stress and inflammatory responses through modulation of Nrf2 and NF-kappaB activation. *Environ Toxicol*. 2021;36(5):926–934. doi:10.1002/tox.23094
- Si Z, Zhang B. Amygdalin attenuates airway epithelium apoptosis, inflammation, and epithelial-mesenchymal transition through restraining the TLR4/NF-kappaB signaling pathway on LPS-treated BEAS-2B bronchial epithelial cells. *Int Arch Allergy Immunol*. 2021;182(10):997–1007. doi:10.1159/000514209
- Niu K, Zhao YJ, Zhang L, Li CG, Wang YJ, Zheng WC. 苦杏仁苷联合羟基红花黄色素A对IL-1β诱导的大鼠椎间盘软骨终板细胞的影响 [The synergistic effect of amygdalin and HSYA on the IL-1beta induced endplate chondrocytes of rat intervertebral discs]. *Yao Xue Xue Bao*. 2014;49(8):1136–1142. Chinese.
- Bian Q, Jain A, Xu X, et al. Excessive activation of TGFbeta by spinal instability causes vertebral endplate sclerosis. *Sci Rep*. 2016;6:27093. doi:10.1038/srep27093
- Ni S, Ling Z, Wang X, et al. Sensory innervation in porous endplates by Netrin-1 from osteoclasts mediates PGE2-induced spinal hypersensitivity in mice. *Nat Commun*. 2019;10(1):5643. doi:10.1038/s41467-019-13476-9
- Miyagi M, Ishikawa T, Kamoda H, et al. Assessment of gait in a rat model of myofascial inflammation using the CatWalk system. *Spine*. 2011;36(21):1760–1764. doi:10.1097/BRS.0b013e3182269732
- Miyagi M, Ishikawa T, Kamoda H, et al. Assessment of pain behavior in a rat model of intervertebral disc injury using the CatWalk gait analysis system. *Spine*. 2013;38(17):1459–1465. doi:10.1097/BRS.0b013e318299536a



30. Boos N, Weissbach S, Rohrbach H, Weiler C, Spratt KF, Nerlich AG. Classification of age-related changes in lumbar intervertebral discs: 2002 Volvo Award in basic science. *Spine*. 2002;27(23):2631–2644. doi:10.1097/00007632-200212010-00002
31. Buckwalter JA. Aging and degeneration of the human intervertebral disc. *Spine*. 1995;20(11):1307–1314. doi:10.1097/00007632-199506000-00022
32. Takahashi K, Aoki Y, Ohtori S. Resolving discogenic pain. *Eur Spine J*. 2008;17(Suppl 4):428–431. doi:10.1007/s00586-008-0752-4
33. Sun HY, Hu KZ, Yin ZS. Inhibition of the p38-MAPK signaling pathway suppresses the apoptosis and expression of proinflammatory cytokines in human osteoarthritis chondrocytes. *Cytokine*. 2017;90:135–143. doi:10.1016/j.cyt.2016.11.002
34. Li Z, Zhang K, Li X, et al. Wnt5a suppresses inflammation-driven intervertebral disc degeneration via a TNF-alpha/NF-kappaB-Wnt5a negative-feedback loop. *Osteoarthritis Cartilage*. 2018;26(7):966–977. doi:10.1016/j.joca.2018.04.002
35. Zhang J, Wang X, Liu H, et al. TNF-alpha enhances apoptosis by promoting chop expression in nucleus pulposus cells: role of the MAPK and NF-kappaB pathways. *J Orthop Res*. 2019;37(3):697–705. doi:10.1002/jor.24204
36. Shirazi-Adl A, Taheri M, Urban JP. Analysis of cell viability in intervertebral disc: effect of endplate permeability on cell population. *J Biomech*. 2010;43(7):1330–1336. doi:10.1016/j.jbiomech.2010.01.023
37. Wang Y, Videman T, Battie MC. ISSLS prize winner: lumbar vertebral endplate lesions: associations with disc degeneration and back pain history. *Spine*. 2012;37(17):1490–1496. doi:10.1097/BRS.0b013e3182608ac4
38. Oichi T, Taniguchi Y, Oshima Y, Tanaka S, Saito T. Pathomechanism of intervertebral disc degeneration. *JOR Spine*. 2020;3(1):e1076. doi:10.1002/jsp2.1076
39. Urits I, Burshtein A, Sharma M, et al. Low back pain, a comprehensive review: pathophysiology, diagnosis, and treatment. *Curr Pain Headache Rep*. 2019;23(3):23. doi:10.1007/s11916-019-0757-1
40. Oichi T, Taniguchi Y, Soma K, et al. A mouse intervertebral disc degeneration model by surgically induced instability. *Spine*. 2018;43(10):E557–E564. doi:10.1097/BRS.00000000000002427
41. Bian Q, Ma L, Jain A, et al. Mechanosignaling activation of TGFbeta maintains intervertebral disc homeostasis. *Bone Res*. 2017;5:17008. doi:10.1038/boneres.2017.8
42. Rade M, Maatta JH, Freidin MB, Airaksinen O, Karppinen J, Williams FMK. Vertebral endplate defect as initiating factor in intervertebral disc degeneration: strong association between endplate defect and disc degeneration in the general population. *Spine*. 2018;43(6):412–419. doi:10.1097/BRS.00000000000002352
43. Xiao ZF, Su GY, Hou Y, et al. Mechanics and biology interact in intervertebral disc degeneration: a novel composite mouse model. *Calcif Tissue Int*. 2020;106(4):401–414. doi:10.1007/s00223-019-00644-8
44. Khan AN, Jacobsen HE, Khan J, et al. Inflammatory biomarkers of low back pain and disc degeneration: a review. *Ann N Y Acad Sci*. 2017;1410(1):68–84. doi:10.1111/nyas.13551
45. Risbud MV, Shapiro IM. Role of cytokines in intervertebral disc degeneration: pain and disc content. *Nat Rev Rheumatol*. 2014;10(1):44–56. doi:10.1038/nrrheum.2013.160
46. Quero L, Klawitter M, Schmaus A, et al. Hyaluronic acid fragments enhance the inflammatory and catabolic response in human intervertebral disc cells through modulation of toll-like receptor 2 signalling pathways. *Arthritis Res Ther*. 2013;15(4):R94. doi:10.1186/ar4274
47. Chen F, Jiang G, Liu H, et al. Melatonin alleviates intervertebral disc degeneration by disrupting the IL-1beta/NF-kappaB-NLRP3 inflammasome positive feedback loop. *Bone Res*. 2020;8:10. doi:10.1038/s41413-020-0087-2
48. Wu X, Liu Y, Guo X, et al. Prolactin inhibits the progression of intervertebral disc degeneration through inactivation of the NF-kappaB pathway in rats. *Cell Death Dis*. 2018;9(2):98. doi:10.1038/s41419-017-0151-z
49. Su X, Liu B, Gong F, et al. Isofraxidin attenuates IL-1beta-induced inflammatory response in human nucleus pulposus cells. *J Cell Biochem*. 2019;120(8):13302–13309. doi:10.1002/jcb.28604
50. Zhu L, Yu C, Zhang X, et al. The treatment of intervertebral disc degeneration using traditional Chinese medicine. *J Ethnopharmacol*. 2020;263:113117. doi:10.1016/j.jep.2020.113117
51. Tang F, Fan K, Wang K, Bian C. Amygdalin attenuates acute liver injury induced by D-galactosamine and lipopolysaccharide by regulating the NLRP3, NF-kappaB and Nrf2/NQO1 signalling pathways. *Biomed Pharmacother*. 2019;111:527–536. doi:10.1016/j.biopha.2018.12.096
52. Zhang A, Pan W, Lv J, Wu H. Protective effect of amygdalin on LPS-induced acute lung injury by inhibiting NF-kappaB and NLRP3 signaling pathways. *Inflammation*. 2017;40(3):745–751. doi:10.1007/s10753-017-0518-4
53. Watkins LR, Maier SF. Implications of immune-to-brain communication for sickness and pain. *Proc Natl Acad Sci USA*. 1999;96(14):7710–7713. doi:10.1073/pnas.96.14.7710